Blue Light-Emitting Diodes Based on Dipyrazolopyridine Derivatives

E. Balasubramaniam,[†] Y. T. Tao,*[,†] A. Danel,[‡] and P. Tomasik[‡]

Institute of Chemistry, Academia Sinica, Taipei, Taiwan, Republic of China, and Department of Chemistry, University of Agriculture, 31 129 Cracow, Poland

Received April 25, 2000. Revised Manuscript Received June 20, 2000

A series of highly luminescent dipyrazolopyridine (PAP) dyes were synthesized and assessed as light-emitting materials in electroluminescent devices. Multilayer devices were fabricated using these dyes along with a hole-transporting material, NPB (4,4′-bis[*N*-(1-naphthyl-1-)-*N*-phenyl-amino]-biphenyl) and an electron-transporting material, AlQ (tris-(8-hydroxyquinoline) aluminum), or TPBI (2,2′,2″-(1,3,5-benzenetriyl)tris[1-phenyl-1H-benzimidazole]). Both ITO/NPB/PAP/AlQ/Mg:Ag and ITO/NPB/PAP/TPBI/Mg:Ag devices gave a bright blue or blue-green emission, depending on the substituent group in the parent PAP dye. The performance of these devices such as turn-on voltage, brightness, and efficiency as a function of the substituent is discussed.

Introduction

Light-emitting diodes (LEDs) using small organic molecules and/or organic polymers are intensively pursued after the initial work by Tang et al.[1] and Friend et al.,[2] apparently due to the potential of using these devices as low-cost alternatives in lighting, back light, and flat panel displays. Much progress has been made in recent years in improving the efficiencies of the electroluminescent (EL) devices through ingenious device configurations, electrode modification, and new material discoveries.[3−5] Numerous fluorescent dyes and charge carriers have been developed, yet the effort is still going on in terms of color tuning, higher efficiency, and durability. Particularly, in the fabrication of multilayer LEDs, optimization of the properties of emitting material and individual charge carriers (electron-transporting material, ETL, and hole-transporting material, HTL) does not necessarily lead to an efficient device. It is important to have the right combination of the electrode materials, charge carriers, and emitting material with appropriate interlayer barriers so that an optimized charge injection and recombination can be achieved.

Among the efforts to achieve different colors, blue light is of particular interest to obtain a white light emission.[6] Because of the wider band gap for the blue emitter, different charge injecting/transporting characteristics may restrict the choice of materials suitable for fabricating a multilayer device.[7−10] Dipyrazolopyridine derivatives are highly fluorescent dyes that exhibit blue emission. Some have been demonstrated to give electroluminescence in polymer device configuration.[11]

In this work, we are reporting a new series of dyes, 1,4,7-triphenyl-3,5-dimethyl-1,7-dihydrodipyrazolo[3,4-b;4′3′-e]pyridine (PAP) as the blue emitting material in a multilayer EL device. Various substituents were introduced at the para position of the 4-phenyl group (Figure 1) and the thermal, spectroscopic, and electrochemical properties were examined. The performances

* To whom correspondence should be addressed.
[†] Academia Sinica.
[‡] University of Agriculture.

(1) Tang, C. W.; Van Slyke, S. A. *Appl. Phys. Lett.* **1987**, *51*, 913.
(2) Burroughes, J. H.; Bradley, D. D. C.; Brown, A. R.; Marks, R. N.; Mackay, K.; Friend, R. H.; Burns, P. L.; Holmes, A. B. *Nature* **1990**, *347*, 539.
(3) (a) Adachi, C.; Tokito, S.; Tsutsui, T.; Saito, S. *Jpn. J. Appl. Phys., Part 2* **1988**, *27*, 269. (b) Tang, C. W.; Van Slyke, S. A.; Chen, C. H. *J. Appl. Phys.* **1989**, *65*, 3610. (c) Hung, L. S.; Tang, C. W.; Mason, M. G. *Appl. Phys. Lett.* **1997**, *70*, 152. (d) Shi, J.; Tang, C. W. *Appl. Phys. Lett.* **1997**, *70*, 1665. (e) Baldo, M. A.; Obrien, D. F.; You, Y.; Shoustikov, A.; Sibley, S.; Thompson, M. E.; Forrest, S. R. *Nature* **1998**, *395*, 104. (f) Uchida, M.; Adachi, C.; Koyama, T.; Taniguchi, Y. *J. Appl. Phys.* **1999**, *86*, 1680.
(4) (a) *Organic Electroluminescent Materials and Devices*; Miyata. S., Nalwa, H. S., Eds.; Gordon and Breach: Amsterdam, 1997. (b) *Acc. Chem. Res.* **1999**, *32*, 191, a special issue on molecular materials in electronics and optoelectronic devices. (c) Ishii, H.; Sugiyama, K.; Ito, E.; Seki, K. *Adv. Mater.* **1999**, *11*, 605.
(5) (a) Shirota, Y. *J. Mater. Chem.* **2000**, *10*, 1. (b) Wu, I.-Y.; Lin, J. T.; Tao, Y.-T.; Balasubramaniam, E. *Adv. Mater.* **2000**, *12*, 668.
(6) (a) Kido, J.; Kimura, M.; Nagai, K. *Science* **1995**, *267*, 1332. (b) Forrest, S. R.; Burrows, P. E.; Shen, Z.; Gu, G.; Bulovic, V.; Thompson, M. E. *Synth. Met.* **1997**, *91*, 9. (c) Xie, Z. Y.; Huang, J. S.; Li, C. N.; Liu, S. Y.; Wang, Y.; Li, Y. Q.; Shen, J. C. *Appl. Phys. Lett.* **1999**, *74*, 641.
(7) (a) Hamada, Y.; Adachi, C.; Tsutsui, T.; Saito, S. *Jpn. J. Appl. Phys.* **1992**, 31, 1812. (b) Hosokawa, C.; Higashi, H.; Nakamura, H.; Kusumoto, T. *Appl. Phys. Lett.* **1995**, 67, 3853. (c) Kido, J.; Kimura, M.; Nagai, K. *Chem. Lett.* **1996**, 47.
(8) (a) Gao, X. C.; Cao, H.; Zhang, L. Q.; Zhang, B. W.; Cao, Y.; Huang, C. H. *J. Mater. Chem.* **1999**, *9*, 1077. (b) Gao, Z. Q.; Lee, C. S.; Bello, I.; Lee, S. T.; Wu, S. K.; Yan, Z. L.; Zhang, X. H. *Synth. Met.* **1999**, *105*, 141.
(9) (a) Noda, T.; Ogawa, H.; Shirota, Y. *Adv. Mater.* **1999**, *11*, 283. (b) Gao, Z.; Lee, C. S.; Bello, I.; Lee, S. T.; Chen, R.-M.; Luh, T.-Y.; Shi, J.; Tang, C. W. *Appl. Phys. Lett.* **1999**, *74*, 865. (c) Mi, B. X.; Gao, Z. Q.; Lee, C. S.; Lee, S. T.; Kwong, H. L.; Wong, N. B. *Appl. Phys. Lett.* **1999**, *75*, 4055. (d) Parthasarathy, G.; Gu, G.; Forrest, S. R. *Adv. Mater.* **1999**, *11*, 907.
(10) (a) Tao, X. T.; Suzuki, H.; Wada, T.; Sasabe, H.; Miyata, S. *Appl. Phys. Lett.* **1999**, *75*, 1655. (b) Hu, N. X.; Esteghamatian, M.; Xie, S.; Popovic, Z.; Hor, A.-M.; Ong, B.; Wang, S. *Adv. Mater.* **1999**, *11*, 1460. (c) Wang, J. F.; Jabbour, G. E.; Mash, E. A.; Anderson, J.; Zhang, Y.; Lee, P. A.; Armstrong, N. R.; Peyghambarian, N.; Kippelen, B. *Adv. Mater.* **1999**, *11*, 1266.
(11) (a) He, Z. Q.; Milburn, G. H. W.; Danel, A.; Puchala, A.; Tomasik, P.; Rasala, D. *J. Mater. Chem.* **1997**, *7*, 2323. (b) Danel, A.; He, Z.; Milburn, G. H. W.; Tomasik, P. *J. Mater. Chem.* **1999**, *9*, 339.

10.1021/cm0003368 CCC: $19.00
Published on Web 08/12/2000

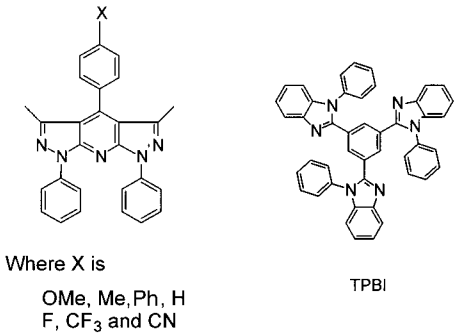

Figure 1. Structures of PAP derivatives and electron-transporting material, TPBI.

of double hetero-junction LED devices of the structures ITO/NPB/PAP/AlQ/Mg:Ag and ITO/NPB/PAP/TPBI/Mg:Ag (with ITO as indium tin oxide, NPB as 4,4′-bis[*N*-(1-naphthyl-1-)-*N*-phenyl-amino]-biphenyl, AlQ as tris-(8-hydroxyquinoline) aluminum, and TPBI as (2,2′,2″-(1,3,5-benzenetriyl)tris[1-phenyl-1H-benzimidazole], respectively) were measured. Exciton formation within the dye layer and blue light emission were established. The performance of the device depends on the 4-substituent so that a higher luminescence and external quantum efficiency was observed for PAPs carrying an electron-rich para substituent at the 4-phenyl group of PAP.

Experimental Section

Materials. The PAP derivatives were prepared according to a literature procedure.[12] The various substituted PAPs were fully characterized by NMR, MS, and comparison with literature data. The TPBI was prepared from benzene-1,3,5-tricarbonyl chloride and *N*-phenyl-1,2-phenylenediamine, followed by dehydration.[13] The NPB and AlQ were prepared via published methods and subject to gradient sublimation prior to use. The substrate was an indium tin oxide- (ITO-) coated glass with a sheer resistance of ∼50 Ω/□.

Device Fabrication. Prepatterned ITO substrates with an effective individual device area of 3.14 mm^2 were cleaned by sonication in a detergent solution for 3 min and then washed with a large amount of doubly distilled water. Further sonication in ethanol for 3 min was done before being blown dry with a stream of nitrogen. The ITO substrates were then treated with oxygen plasma for 1 min before being loaded into the vacuum chamber. The organic layers were deposited thermally at a rate of 0.1−0.3 nm/s under a pressure of 2×10^{-5} Torr. Devices were constructed with 40-, 7.5-, and 15-nm thickness of NPB, PAP dye, and AlQ, respectively, for ITO/NPB/PAP/AlQ/Mg:Ag devices. As pyrazoline derivatives have been reported[14] to be hole-transporting, a 15-nm thickness of AlQ was chosen, which turned out to give pure blue emission for all cases except the PAP−CN derivative. In the case of ITO/NPB/PAP/TPBI/Mg:Ag devices the thicknesses of the organic layers were 40, 6, and 40 nm for NPB, PAP dye, and TPBI, respectively. Then, 50 nm of an Mg:Ag cathode alloy (∼10:1 ratio) was deposited by coevaporation. Finally, a capping layer of Ag (100-nm thick, deposition rate of 0.1−0.4 nm/s) was deposited on the device.

Instrumentation. The thermal data were obtained from a Perkin-Elmer DSC7 differential scanning calorimeter, which is equipped with an insulated reservoir for the use of a coolant. Absorption and emission measurements were done using Hewlett-Packard 8453 absorption and Hitachi F-4500 fluorescence spectrophotometers, respectively. Emission quantum yields were measured with reference to Coumarin 1 dye (7-diethylamino-4-methylcoumarin) in ethyl acetate.[15] The thermal evaporation of organic materials was carried out using ULVAC Cryogenics at a chamber pressure of 10^{-5} Torr. The layer thickness was monitored by a Maxtek TM200 quartz crystal. Current−voltage−light intensity (I−V−L) of LEDs were measured using a Keithley 2400 source meter and a Newport 1835C multifunction optical meter, equipped with a silicon photodiode (Newport, model 818-ST). The measurements of I−V−L were performed simultaneously through an IEEE interface to a computer. All the measurements were made at atmospheric conditions. Cyclic voltammetric experiments were done using a BAS 100B electrochemical analyzer. A three-electrode cell system with a glassy carbon, a platinum wire, and a silver wire as the working, counter, and reference electrode, respectively, was used, while 0.1 M tetrabutylammonium hexafluorophosphate was a supporting electrolyte and freshly distilled, degassed dichloromethane was used as the solvent.

Results and Discussion

Thermal Studies. As a general trend, the PAP dyes possess high melting points and high crystallization temperatures (Table 1). Thermal gravimetric analysis (TGA) showed that these dyes are stable up to 420 °C. Differential scanning calorimetry (DSC) showed that only phenyl-substituted PAP (PAP−Ph) dye exhibits a glass transition temperature, T_g, at around 88 °C. Upon the first heating cycle, only a melting temperature, T_m, was observed at 255 °C. After the sample cell was quenched with liquid nitrogen, a second heating cycle exhibited a T_g value (Figure 2), followed by the crystallization temperature T_c and the melting temperature T_m.

Absorption Spectra and Photoluminescence. The absorption spectra of PAP dyes in ethyl acetate and the spectra data are summarized in Table 1. In all the cases, an intense absorption covers the entire range from 250 to 400 nm. The molar extinction coefficient is on the order of 5 in the high-energy region and the same is on the order of 4 for absorption around 376 nm, the low-energy region. The same spectral pattern was observed for differently substituted derivatives. However, there is a slight shift in the peak maximum, i.e., the absorption shifts to a longer wavelength in going from an electron-donating methoxy-substituted (PAP−OMe) to electron-withdrawing cyano-substituted (PAP−CN) derivative, by about 4−9 nm for various peaks. The photoluminescence (PL) spectra of PAP dyes in ethyl acetate are shown in Figure 3 and the peak positions are given in Table 1. A similar substituent effect was also found for the emission peak maximum; that is, the emission maximum shifts to a longer wavelength on going from derivatives substituted with an electron-donating group to ones substituted with an electron-withdrawing group. Thus, the PAP−OMe has an emission peaked at 426 nm, whereas the PAP−CN has an emission peaked at 463 nm. The relative quantum yields were measured in ethyl acetate using Coumarin 1 dye as the reference. The quantum yields, as summarized in Table 1, range between 0.43 for PAP−CF_3 and 0.89 for PAP−OMe. The solid state PL spectra were measured for thin films of PAP dyes evaporated on a glass substrate, as shown in Figure 4. The solid PL spectra

(12) Hennig, L.; Hofmann, J.; Alva-Astudillo, M.; Mann, G. *J. Prakt. Chem.* **1990**, *332*, 351.

(13) (a) Shi, J.; Tang, C. W.; Chen, C. H. U.S. Patent 5,645,948, 1997. (b) Chen, C. H.; Shi, J. *Coord. Chem. Rev.* **1998**, *171*, 161.

(14) (a) Sano, T.; Fujii, T.; Nishio, Y.; Hamada, Y.; Shibata, K.; Kuroki, K. *Jpn. J. Appl. Phys. Part 1* **1995**, *34*, 3124. (b) Borsenberger, P. M.; Schein, L. B. *J. Phys. Chem.* **1994**, *98*, 233. (c) Young, R. H.; Fitzgerald, J. J. *J. Phys. Chem.* **1995**, *99*, 4230.

Table 1. Thermal and Spectral Characteristics of PAP Materials

	PAP−OMe	PAP−Me	PAP−H	PAP−Ph	PAP−F	PAP−CF_3	PAP−CN
formula	$C_{28}H_{23}N_5O$	$C_{28}H_{23}N_5$	$C_{27}H_{21}N_5$	$C_{33}H_{25}N_5$	$C_{27}H_{20}N_5F$	$C_{28}H_{20}N_5F_3$	$C_{28}H_{20}N_6$
melting point, °C	216−219	250−253	230−233	250−252	229−231	245−247	260−262
crystallization temperature, °C	185	216	180	178/114[a]	174	188	205
T_g, °C	N.A.	N.A.	N.A.	88	N.A.	N.A.	N.A.
absorption maxima, nm	257, 277, 330, 362	258, 277, 330, 362	259, 277, 330, 363	258, 276, 331, 367	260, 277, 330, 367	260, 278, 332, 369	263, 282, 334, 371
emission peak, nm (solution)	426	430	433	440	433	447	463
emission peak, nm (solid film)	438	437	435	443	440	449	466
relative quantum yield	0.76	0.76	0.68	0.89	0.58	0.43	0.50

[a] During heating cycle.

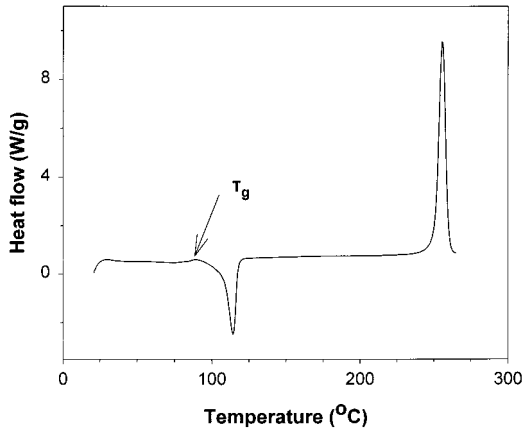

Figure 2. DSC curve for PAP−Ph at the scan rate of 20 °C/min (second heating cycle).

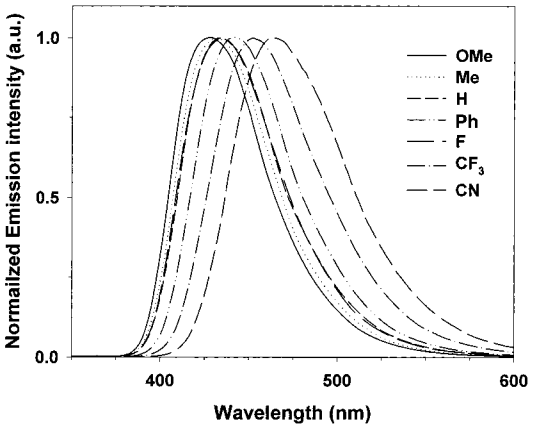

Figure 3. Normalized solution PL spectra of PAP materials in ethyl acetate. The absorption peak around 330 nm was chosen as the excitation wavelength for all PAP dyes.

are slightly broadened relative to the solution PL spectra. For PAP−OMe a 12-nm red shift was observed in the solid film as compared to that of the solution PL, while the shifts for other derivatives are smaller (Table 1). The small shifts imply that there is little excimer formation in the thin film state. Molecular mechanic calculation showed that the 4-phenyl ring is nearly perpendicular to the dipyrazolopyridine moiety and the two phenyl rings on the 4- and 7-position are also twisted by about 40° from the same moiety. This geometry may well prevent the excimer formation. From the above observations, it was suggested that the PAP dyes might be suitable for LED purposes.

Electrochemistry. The redox properties as well as the HOMO (highest occupied molecular orbital) and LUMO (lowest unoccupied molecular orbital) energy

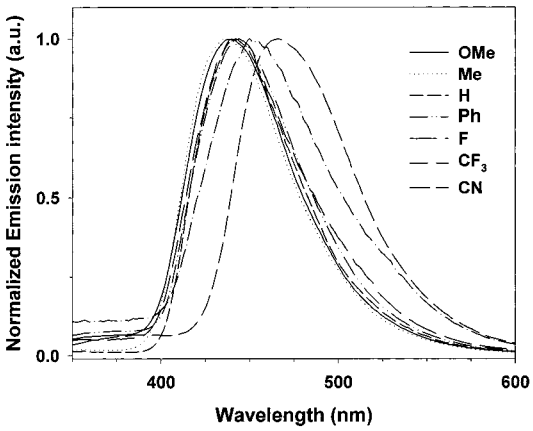

Figure 4. Normalized solid PL spectra of PAP materials on glass. The excitation wavelength was kept around 330 nm.

levels of the materials are crucial parameters for LED configuration. Usually, the ionization potential (IP, i.e., the HOMO of an organic molecule) is measured by ultraviolet photoelectron spectroscopy (UPS), while the electron affinity (EA, i.e., the LUMO of the organic molecule) is deduced from the IP value and the band gap, which is obtained from the absorption edge of optical absorption spectra.[16] The oxidation potential, as determined by cyclic voltammetry (CV), is related to the IP and offers an alternative approach to obtain the HOMO/LUMO energy levels.[16,17] It is a simple and useful technique to compare the relative energy levels for the series of derivatives in the same class.

All PAP dyes exhibit an irreversible oxidation peak at the glassy carbon electrode with reference to the Ag/AgCl electrode. Table 2 lists the oxidation potentials of the PAP dyes. Apparently, the substituent group on the 4-phenyl ring has little effect on the oxidation potential (E_{ox}), which occurs around $+1.56 \pm 0.01$ V. The HOMO energy level is calculated according to the equation reported by Janietz et al,[16] with IP $= (E_{OX} + 4.4)$ eV and the LUMO energy level is obtained by subtraction of the optical band gap from the IP. The summary of HOMO and LUMO energy levels of PAP dyes is given in Table 2. Thus, all the PAP dyes have similar HOMOs. It is also noted that the band gaps of the PAP dyes are also similar, except the PAP−CN, which has a smaller band gap due to a larger red shift in the optical absorption spectra. The low sensitivity of the oxidation

(15) Jones, G., II; William, W. R.; Jackson, R.; Choi, C. Y.; Bergmark, W. R. *J. Phys. Chem.* **1985**, *89*, 294.
(16) Janietz, S.; Bradley, D. D. C.; Grell, M.; Giebeler, C.; Inbasekaran, M.; Woo, E. P. *Appl. Phys. Lett.* **1998**, *73*, 2453.
(17) (a) Thelakkat, M.; Schmidt, H.-W. *Adv. Mater.* **1998**, *10*, 219. (b) Koene, B. E.; Loy, D. E.; Thompson, M. E. *Chem. Mater.* **1998**, *10*, 2235.

Table 2. Energy Alignment in PAP Materials

	E_{ox}, V[a]	HOMO, eV[a]	band gap, eV[a]	LUMO, eV
PAP−OMe	1.56	5.96	3.10	2.86
PAP−Me	1.57	5.97	3.10	2.87
PAP−Ph	1.56	5.96	3.09	2.87
PAP−H	1.57	5.97	3.09	2.88
PAP−F	1.57	5.97	3.10	2.87
PAP−CF_3	1.56	5.96	3.08	2.88
PAP−CN	1.55	5.95	2.85	3.10
ITO		4.70 (E_F)		
NPB	0.83	5.23	3.03	2.20
AlQ[b]		6.09		2.95
TPBI[c]	1.80	6.20	3.50	2.70
Mg:Ag				3.70 (E_F)

[a] Please see the text. [b] Reference 8a. [c] Reference 8b.

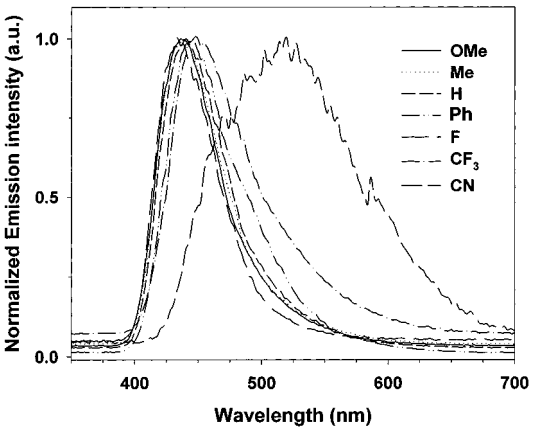

Figure 5. Normalized electroluminescence spectra of ITO/NPB/PAP/AlQ/Mg:Ag devices. The applied voltage was around 9 V.

potential as well as absorption frequency toward the substituent may relate to the structure of the PAP. The phenyl group carrying the substituent is nearly perpendicular to the dipyrazolopyridine unit and thus conjugation with the parent moiety is small. Table 2 also shows the HOMO and LUMO energy levels of other materials involved in this study. From the energy alignment, it is suggested that charge injection into the dye layer for a three-layer electroluminescent device is feasible.

Electroluminescence. The strong fluorescence exhibited by the PAP dyes both in solution and solid state as well as the electrochemical studies suggest that these materials are suitable candidates for fabricating a light-emitting device. A three-layer device configuration was examined, where the PAP dyes were the emission layer and the NPB was the hole transporter. Either AlQ or TPBI was used as the electron transporter. All seven PAP dyes were tested in fabricating the ITO/NPB/PAP/AlQ/Mg:Ag device while three representative compounds (those with a strong electron-donating 4-methoxy group (PAP−OMe), a weak electron-donating phenyl group (PAP−Ph), and a strong electron-withdrawing cyano group (PAP−CN)) were examined with ITO/NPB/PAP/TPBI/Mg:Ag structure.

(a) ITO/NPB/PAP/AlQ/Mg:Ag Devices. With the same configuration ITO/NPB(40 nm)/PAP(7.5 nm)/AlQ-(12.5 nm)/Mg:Ag(50 nm), all devices gave a bright blue emission whereas the PAP−CN device gave a weak blue-green emission. Figure 5 depicts the normalized EL spectra of all seven devices. The PAP−CF_3 gave a emission maximum at 448 nm and PAP−OMe gave a maximum at 436 nm, values which are very close to the solid-state PL values of 449 and 438 nm, respectively. The same substituent dependence in the EL and PL implies that the emission originated from the dye layer, which in turn suggests that the charge recombination occurred at the dye layer. The different Commission Internationale de L'Eclairage (CIE) coordinates (*x* and *y* values, respectively) (Table 3) for different substituents further confirm the emission from PAP dyes. The device with PAP−CN as the emission layer showed a blue-green light with a much broader EL that peaked around 520 nm with a shoulder at around 460 nm; CIE coordinates, *x* and *y*, are 0.28 and 0.41, respectively. This indicates that much of the light came from AlQ, while some emission originated from PAP−CN.

The current−voltage (I−V) curves and luminescence plots of ITO/NPB/PAP/AlQ/Mg:Ag devices are shown in Figure 6, parts a and b, respectively. Table 3 summarizes the overall performance of the devices. In general, the turn-on voltages for PAP dyes are ∼4 V or less. The PAP−H and PAP−Ph gave a peak brightness over 4000 cd/m^2 whereas others are lower. While the brightness at a particular current was being compared, the PAP−Ph-based LED gave a higher luminance. The EL external quantum efficiency shows a substituent effect, i.e., more efficient with an electron-donating substituent. This trend is in accord with the relative quantum yield of PAP dyes in solution. The overall power efficiency ranges between 0.1 and 0.5 lm/W at 100 mA/cm^2, which also shows a similar substituent dependence. The EL and performance of a PAP−CN-based device are distinct from that of other PAP dyes. Further discussion pertaining to the PAP−CN device will be given in the following section.

(b) ITO/NPB/PAP/TPBI/Mg:Ag Devices. Figure 7 shows the normalized EL spectra of ITO/NPB(40 nm)/PAP(6 nm)/TPBI(40 nm)/Mg:Ag devices and the emission ranges from 350 to 600 nm. For PAP−OMe, the emission maximum occurs at 440 nm, together with a small shoulder at 375 nm. For PAP−Ph, the emission maximum occurs at 448 nm, again with a shoulder at 375 nm of higher relative intensity. For the PAP−CN device, further red shift of the emission maximum to 462 nm is observed, with further growth of the shoulder at 375 nm. Again, the dependence of the emission maximum on the substituent group is similar to that observed in the PL of the solid film of these dyes, which implies the emission comes from the dye layer. However, the common shoulder observed in each spectrum, attributable to the emission from TPBI,[18] indicates some holes leaked into the TPBI layer to form a singlet exciton there. The CIE coordinates (*x* and *y* values, respectively) for PAP−OMe, PAP−Ph, and PAP−CN devices are (0.17, 0.12), (0.15, 0.12), and (0.18, 0.22), respectively. The CIE coordinate values for devices with PAP−OMe or PAP−Ph as the emission material are nearly similar whether AlQ or TPBI are used as the electron-transporting layer. The small drop in the CIE *x*, *y* value may reflect the presence of the shoulder at 375 nm in the case of the TPBI device.

It is interesting to note the relative increase of the shoulder peak for TPBI at around 375 nm in the EL for

(18) Tao, Y.-T.; Balasubramaniam, E.; Danel, A.; Tomasik, P. *Appl. Phys. Lett.*, in press.

Table 3. Performance of the LEDs Fabricated in This Study

	turn-on voltage, V	voltage, V (*at 100 mA/cm^2)	brightness*, cd/m^2	quantum efficiency*, %	power efficiency*, lm/W	CIE coordinates *x* and *y*
			(i) ITO/NPB/PAP/A1Q/Mg:Ag Devices			
PAP−OMe	3.0	5.1	761	0.84	0.46	0.18 and 0.11
PAP−Me	3.9	5.4	757	0.84	0.45	0.18 and 0.12
PAP−H	4.0	5.5	739	0.80	0.43	0.17 and 0.11
PAP−ph	4.2	6.4	850	0.72	0.39	0.16 and 0.13
PAP−F	4.1	5.4	415	0.51	0.23	0.18 and 0.10
PAP−CF_3	4.0	5.8	413	0.28	0.22	0.20 and 0.19
PAP−CN	3.0	4.9	155	0.06	0.10	0.28 and 0.41
			(ii) ITO/NPB/PAP/TPBI/Mg:Ag Devices			
PAP−OMe	3.4	6.9	1112	1.26	0.51	0.17 and 0.12
PAP−ph	3.5	6.6	997	1.02	0.46	0.15 and 0.12
PAP−CN	3.5	6.1	399	0.25	0.19	0.18 and 0.22

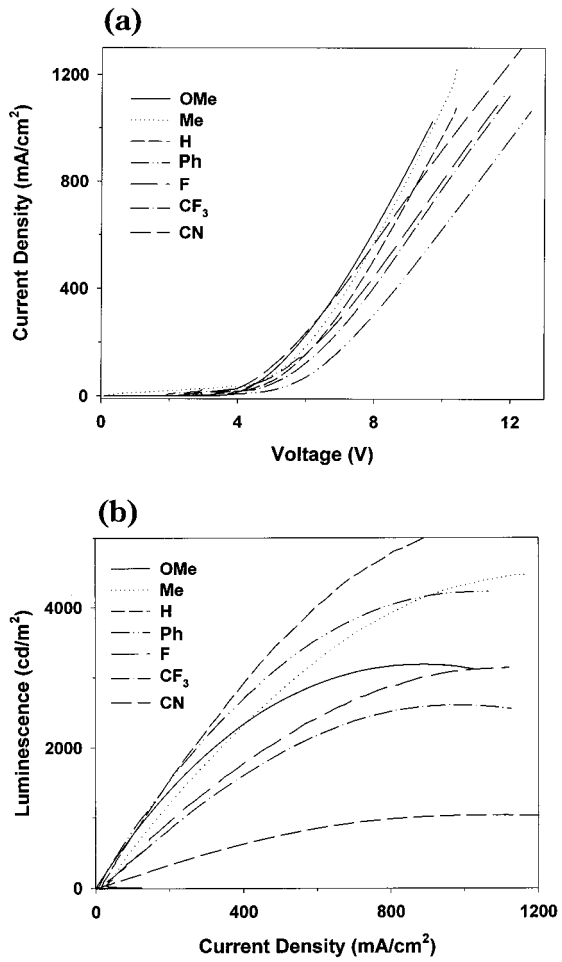

Figure 6. (a) Current density−voltage and (b) luminescence−current density characteristics of ITO/NPB/PAP/AlQ/Mg:Ag devices.

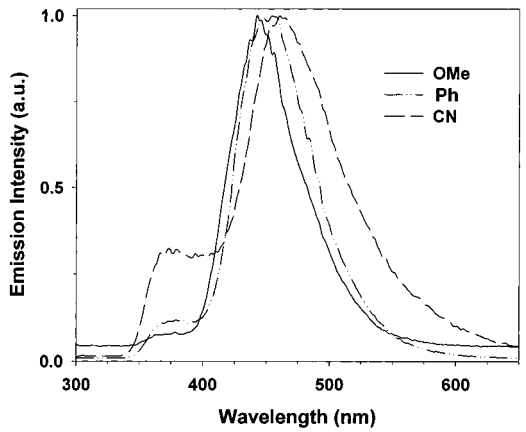

Figure 7. Normalized electroluminescence spectra of ITO/NPB/PAP/TPBI/Mg:Ag devices. The applied voltage was around 9 V.

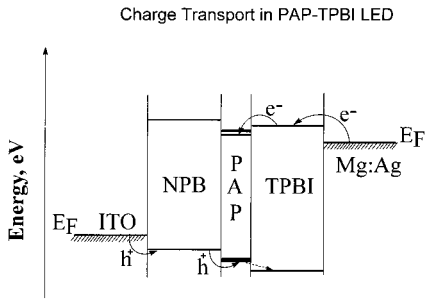

Figure 8. Relative energy alignments in the ITO/NPB/PAP/TPBI/Mg:Ag device.

the three ITO/NPB/PAP/TPBI/Mg:Ag devices. The emission ratio of $\lambda_{375}/\lambda_{max}$ (defined as the area ratio under the peak at 375 nm and the major emission around 450 nm) was found to increase on going from PAP−OMe to PAP−Ph and PAP−CN, the order of decreasing electron density for the substituent. Since the PAP layer is 6 nm in thickness, it is unusual for tunneling injection of holes from NPB layer to TPBI layer to occur and this fact is further confirmed by increasing the emission layer thickness to 10 nm where the relative intensity of the TPBI emission is not decreased. Thus, the holes were transferred through the PAP layer. With the current device structure, the only variable is the identity of the emission material. Figure 8 shows the energy level diagram for various ITO/NPB/PAP/TPBI/Mg:Ag devices. However, the HOMO levels for all PAP dyes are similar; thus, the barrier encountered when the hole travels through to the TPBI layer should be similar in devices with different dyes. There is a difference in the LUMO levels for various dyes, ∼0.2 eV lower with PAP−CN versus that of the other two. Nevertheless, all LUMO energy levels of PAP dyes are lower than that of TPBI, and thus the transfer of an electron from TPBI is presumed as the same. The observed higher proportion of TPBI emission in a PAP−CN-based device may suggest more hole leakage into the TPBI for this material. A possible cause is a different hole mobility for this PAP−CN derivative. A higher leakage of holes into the ETL was also observed in the NPB/PAP−CN/AlQ/Mg:Ag device as described earlier. Indeed, the pyrazoline-based material has been reported[14] to be hole-transporting.

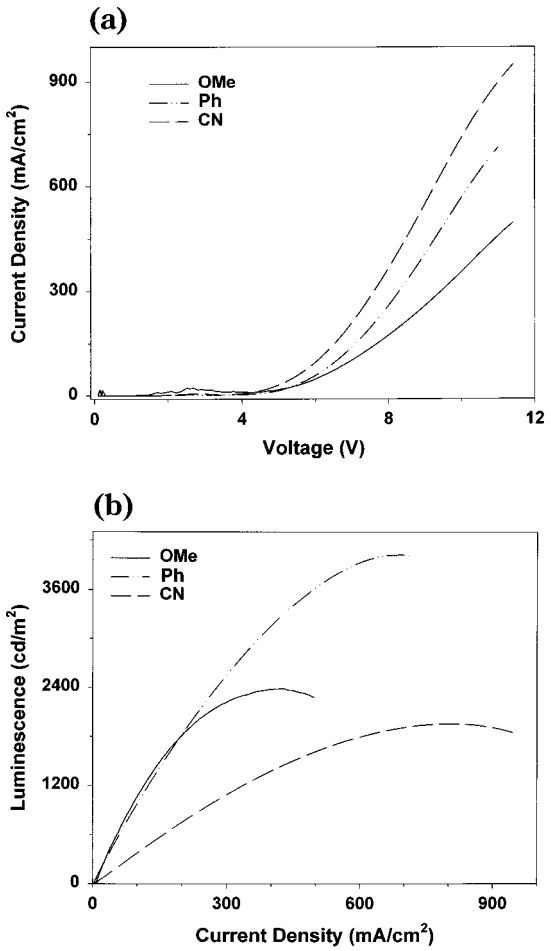

Figure 9. (a) Current density−voltage and (b) luminescence−current density characteristics of ITO/NPB/PAP/TPBI/Mg:Ag devices.

The I−V−L plots for ITO/NPB/PAP/TPBI/Mg:Ag devices are shown in Figure 9, parts a and b. The turn-on voltage is around 3.5 V. The luminescence of PAP−OMe, PAP−Ph, and PAP−CN devices are 2400, 3800, and 1800 cd/m^2, respectively, at their peak position, which is a trend similar to that of ITO/NPB/PAP/AlQ/Mg:Ag devices. Table 3 summarizes the overall performance of the devices. PAP bearing a strong electron-donating substituent, −OMe, or a weak electron-donating Ph− group shows a better performance than that with an electron-withdrawing substituent, −CN. The lower performance of a PAP−CN-based device may be due to the lower quantum yield of the dye as well as poor confinement of the charge recombination.

Conclusions

In conclusion, a new series of dipyrazolopyridine dyes have been evaluated as emitting material in fabricating EL devices. Bright blue emission from the dye can be obtained in a double-heterojunction device structure with NPB as the hole-transporting layer and either AlQ or TPBI as the electron-transporting layer. The performance of the device depends on the substitution on the PAP dye. Higher external quantum efficiency and power efficiency were found for PAP dyes substituted with electron-donating groups. Lower efficiency with cyano-substituted PAP dye may be attributed to lower quantum yield of the dye as well as the poor charge confinement. With AlQ as the electron-transporting layer, peak luminescence ranging between 1000 and 5000 cd/m^2 was observed, depending on the substituent. Power efficiency ranging from 0.10 to 0.46 lm/W and the external quantum efficiency ranges from 0.06% to 0.84% were obtained. With TPBI as the electron-transporting material, the peak luminescence ranging between 1800 and 3800 cd/m^2 and a power efficiency ranging between 0.19 and 0.51 lm/W and the external quantum efficiency of ∼1% except for PAP−CN were obtained, depending again on the substitution.

Acknowledgment. Y.T.T. and E.B. would like to thank China Petroleum Corporation and Academia Sinica, Republic of China, for financial support. P.T. and A.D. would like to thank the Polish Scientific committee for financial support.

CM0003368